

Spherical Aerial Manipulator Robot for Exploration in Complex Forest Environments

J. Daniel Olivares-Figueroa, Israel Cruz-Vega *, Alejandro Gutierrez-Giles, and Jose Martinez-Carranza
 Insituto Nacional de Astrofisica, Optica y Electronica - Puebla, Mexico

ABSTRACT

One significant research area that has greatly benefited from UAVs is precision agriculture, due to their ability to offer excellent spatial resolution, making them ideal for detailed minor-scale analyses of vegetable patches. To the best of our knowledge, few studies have applied UAVs to explore complex forest environments, such as orchards, often relying on indirect methods to obtain crop information. In this work, we propose a novel approach that enables the direct measurement of characteristics, such as individually measuring fruits or stems/leaves, to assess their maturity or detect crop diseases, respectively. To achieve this, we introduce a new design called “SAMBot: Spherical Aerial Manipulator Robot”, which consists of a mini-UAV protected by a spherical structure with an attached manipulator at its front. SAMBot combines the protective benefits of the spherical design with the manipulator’s ability to access confined spaces. The proposed design is compatible with ROS2, a widely-used framework in robotics research and industrial applications. The range of potential applications for our proposed design extends beyond precision agriculture, encompassing areas such as search and rescue operations in mines or collapsed buildings, structural inspections, and autonomous underground navigation, among others.

1 INTRODUCTION

Unmanned Aerial Vehicles (UAVs), or drones, are aeronautical complex systems that can be controlled without an onboard pilot for autonomous flights. Due to the integration of advanced navigation systems with cameras and sensors, it is possible to collect data for various tasks such as space, sea, and land exploration, as well as numerous applications in the entertainment and military industries, among others [1, 2].

Precision Agriculture (PA) is one of the scientific fields that has most benefited from UAV technology. The increase in the world population and the extreme weather events caused by global warming are making food production in-

creasingly challenging [3]. Drones offer a potential solution to these challenges by improving agricultural efficiency and productivity through crop monitoring, irrigation management, pesticide and fertilizer spraying, cartography, and more [4, 5].

While drone research in precision agriculture has led to significant advancements, it is essential to acknowledge the current limitations. Most studies primarily focus on acquiring images and geospatial data to estimate overall crop health. Drones are restricted to flying over orchards at a specific altitudes to capture thermal, multispectral, or RGB images. While effective for global data estimation, this approach does not facilitate the acquisition of local data. In [6], the exploration of a drone through an apple orchard is presented, using an indirect technique to determine fruit maturity by detecting ethylene in the air. In [7], a UAM is used to install and recover sensors in trees, preventing fires through the real-time monitoring. The manipulator has a single prismatic joint for surface contact, which limits its accuracy for other applications. In [8], a UAV installs a sensor network in forests to measure temperature, pressure, and luminosity. The authors do not incorporate a manipulator; instead, the drone is positioned 3 meters from the target to launch the sensors. In [9], a UAM with two passive rotating hemispherical shells is presented for manipulating objects in complex environments during disasters. However, the manipulator is mounted on the drone body, has a single degree of freedom (DoF), and only extends up to 70 mm. We have not found a satisfactory solution that allows for the direct measurement of orchard characteristics, such as assessing individual fruits or stems/leaves to determine their maturity or detect crop diseases.

The importance of obtaining precise information on the ripeness state of each fruit lies in the ability to determine the optimal harvest time, assess the number of days required to reach the optimal ripeness for consumption, and apply treatments to slow down the maturation process during export. Traditional methods are time-consuming and involve premature destruction of the fruits, leading to economic losses. Furthermore, these methods rely on a small sample size to estimate the conditions of the entire orchard.

In this article, we propose the design of a mini-quadcopter protected by a lightweight and resistant spherical casing and equipped with a robotic arm called “SAMBot: Spherical Aerial Manipulator Robot.” This proposal addresses the identified problem by combining the protective advantages of the spherical casing in complex environments (such as tree

*Email address(es): icruzv@inaoep.mx



Figure 1: (a) Design for underground applications. (b) Obstacle detection with ultrasound. (c) Detection of workers in mines using the camera [11].

branches or leaves) with the manipulator’s capability to access confined spaces. We present several challenges encountered during the simulation phase of SAMBot’s design. Concurrently, we have been developing the physical design, considering challenges such as ensuring the combined weight of the sphere and manipulator does not exceed the drone’s lifting capacity, and accounting for changes in the center of mass due to the manipulator’s position, among other factors, to implement this design as a new entity in the Gazebo software while adhering to physical constraints.

Although we have not found in the literature a similar work, we now present some related works on spherical drones and aerial manipulators. A spherical drone (SD) is equipped with a spherical structure that provides protection and allows it to access confined and hazardous spaces without compromising the integrity and stability of the drone and its environment [10]. In [11], the SD is trained using deep learning techniques to fly in dangerous environments without GPS, such as mines for workers’ rescue missions. Figure 1 shows some examples. Other tasks, such as autonomous underground navigation, survivor search, and infrastructure inspection, are considered in [12]. In [10] and [13], a drone is designed with a passive rotating spherical cage mechanism to stabilize it during collisions with structures damaged by earthquakes, fires, or explosions, such as buildings and bridges. In [14], this system employs cameras with computer vision and machine learning techniques to map public spaces and track city pedestrian flow. In [15], a cargo drone with a foldable modular spherical structure is used to lift packages weighing up to 500 grams. Authors in [16] present a more visually appealing application, where the drone casing creates three-dimensional images through the synchronized rotation and activation of multiple LED ribbons, arcing around the sphere to create virtual and augmented reality experiences, displaying 3D images for telepresence applications.

An Unmanned Aerial Manipulator (UAM) is a robotic system consisting of a drone equipped with a multi-DoF manipulator and various sensors and tools, such as claws or grippers. Its use expands the drone’s ability to complete complex tasks and enhances the manipulator’s maneuverability [17]. Since UAMs are the systems most similar to SAMBot, we have conducted an exhaustive search of the state-of-the-art UAMs [17–37]. According to these works, the most com-

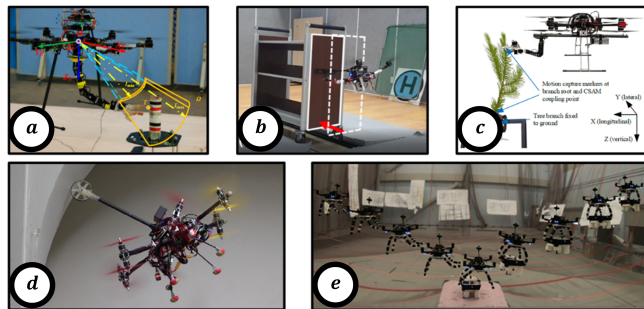


Figure 2: Featured applications of the UAM. (a) Grip/Placement. (b) Contact with quasi-static surface. (c) Coupling between the UAM and the object. (d) Contact with static surface. (e) Dynamic grip.

mon applications for UAMs include trajectory tracking, position/orientation control, grasping and placement tasks, contact tasks, and force control (see Figure 2). The quadcopter is the most used UAV for UAMs, followed by the hexacopter and octocopter. 2-DoF manipulators are the most frequently used for equipping drones, as these systems are lighter and more compact in terms of weight and size. Furthermore, by leveraging the DoFs of the UAV itself, a more complex manipulator is not always necessary for certain tasks.

To obtain a mathematical description of UAMs, the Euler-Lagrange formulation is the most commonly used method for expressing the dynamic model, followed by the Newton-Euler formulation and the Recursive Newton-Euler formulation. Approximately 61% of the reviewed articles use a decoupled method, treating the manipulator as an additional disturbance. Additionally, we found that the control technique most commonly used for UAMs is PID control due to its straightforward design and implementation. Although the best results are not always achieved, most authors report that its performance is adequate for specific applications. Other techniques, such as Robust and Adaptive Control, are employed in more complex applications along with the use of a nonlinear dynamic model.

The rest of the paper is organized as follows: Section 2 provides a description of our proposed system and discusses the mathematical model for PID control actions, which represents an initial approach to controlling the drone in desired positions. Section 3 presents details of the design and results of the PID control. Finally, Section 4 summarizes the findings of this study and the future tendencies.

2 METHODOLOGY AND DESIGN

2.1 Description of the System

SAMBot consists of a drone protected by a spherical structure, equipped with a 3 DoF manipulator, capable of positioning and orienting its end-effector in the plane. The actuators in the design correspond to the MG90S servomotor.

http://www.imavs.org/

The manipulator has three MPU6050 IMU sensors attached to each joint. Unlike an encoder, data acquisition with the IMU is simpler and does not require additional electronics nor direct mounting on the joint motor shaft, which makes it easier to install on a smaller and lighter structure that is useful in mobile applications such as drones. The end effector has an ESP32–Cam camera to estimate distances and implement computer vision techniques in future applications and a VL53L0X distance sensor near the camera lens to corroborate the measurements.

Since the payload for most mini-drones is very limited, all the components mentioned above were carefully selected to maintain the payload to the minimum while still having the necessary components to perform the tasks commonly presented in most PA scenarios. The spherical casing design, including the volume of the casing and the material selection, was as well iteratively designed to maintain the payload to the minimum. Moreover, the arm manipulator is incorporated to be part of the spherical casing to further reduce the payload.

According to [38], the dynamic equations of the quadcopter as a mechanical system are obtained using Newton’s laws. Then the quadcopter motion is described by a non-linear system of six differential equations. Also considering the mathematical equations of a planar revolute joint manipulator and supposing an n -link robot attached to the drone, the mathematical model of the manipulator is obtained using Euler-Lagrange formalism. After considering the manipulator connected to the quadcopter, values of the elements in the inertia tensor are changed due to the additional inertia of the manipulator links, the moment of inertia generated by each material point resulting in an inertia tensor of the combined system, also is determined the mutual influence between the quadcopter and the manipulator, considering the position displacement of the mass center of the combined system and the torque reaction forces $\tau_{(x,y,z)}$ acting on the quadcopter from the manipulator. The mathematical model of the quadcopter is described by the equations:

$$\begin{cases} m_m \ddot{x} = (s_\psi s_\phi + c_\psi s_\theta c_\phi)F + d_1 \\ m_m \ddot{y} = (-c_\psi s_\phi + s_\psi s_\theta c_\phi)F + d_2 \\ m_m \ddot{z} = -m_m g + (c_\theta c_\phi)F + d_3 \\ I_{xx} \ddot{\phi} = (I_{yy} - I_{zz})\dot{\theta}\dot{\psi} - I_{xz}(\dot{\phi}\dot{\theta} + \ddot{\psi}) + \tau_x + d_4 \\ I_{yy} \ddot{\theta} = (I_{zz} - I_{xx})\dot{\phi}\dot{\psi} + I_{xz}(\dot{\phi}^2 - \dot{\psi}^2) + \tau_y + d_5 \\ I_{zz} \ddot{\psi} = (I_{xx} - I_{yy})\dot{\phi}\dot{\theta} + I_{xz}(\dot{\theta}\dot{\psi} + \ddot{\phi}) + \tau_z + d_6 \\ \mathbf{M}(\mathbf{q})\ddot{\mathbf{q}} + \mathbf{C}(\mathbf{q}, \dot{\mathbf{q}}) + \mathbf{g}(\mathbf{q}) + \mathbf{d}_7 = \boldsymbol{\tau} \end{cases} \quad (1)$$

where s_x and c_x denotes $\sin(x)$ and $\cos(x)$, respectively; m_m is the overall mass of the whole system; $\ddot{x}, \ddot{y}, \ddot{z}$ are the linear accelerations of the quadcopter with respect to the inertial reference frame; I_{xx}, I_{yy}, I_{zz} represents the inertia tensor of the combined system; ψ, θ, ϕ are the *Yaw – Pitch – Roll* angles that describe the drone orientation, angular velocity $(\dot{\psi}, \dot{\theta}, \dot{\phi})$ and angular acceleration $(\ddot{\psi}, \ddot{\theta}, \ddot{\phi})$; F is the lift of the airframe; τ_x, τ_y, τ_z are the torques of the three axes of the airframe, respectively; I_{xz} represents the inertia product of the

combined system (since the manipulator operates on $x - z$ plane); g is the gravitational acceleration constant. For the manipulator: $\mathbf{M}(\mathbf{q})$ is the inertia matrix; $\mathbf{C}(\mathbf{q}, \dot{\mathbf{q}})$ is the coriolis and centripetal forces matrix; $\mathbf{g}(\mathbf{q})$ is the vector accounting for gravitational forces; $\mathbf{q}, \dot{\mathbf{q}}, \ddot{\mathbf{q}}$ are the vector of generalized coordinates, velocities and accelerations of the manipulator joints, respectively; and $\boldsymbol{\tau}$ are the actuators’ torques. Finally $d_i (i = 1, \dots, 6)$ represents the external disturbance in each channel, and $\mathbf{d}_7 = [d_{71}, \dots, d_{7n}]$ indicates the external interference of the n -link of the manipulator, which the quadcopter and external environment may cause.

2.2 Experimental Simulation Tests

The SAMBot was designed in SolidWorks, and the URDF (Unified Robot Description Format) file was exported using the sw2urdfSetup.exe plugin. The URDF has subsequently been modified to a .urdf.xml format for incorporation with the Parrot AR Drone 2.0 in the sjtu-drone-quadcopter-simulation in Gazebo and communication using ROS2 Humble, installed in Ubuntu 22.04. During this stage, some modifications were realized to join the system with the proper dimensions, mass parameters, and inertia tensor of the links, the joint type, and the action limits. In this sense, we have ensured a faithful representation of the proper conditions to evaluate the drone’s performance in the planned tasks.

To obtain these physical parameters, the mass of each element was first estimated in Ultimaker-Cura-5.2.1, using the PLA material with a density of 25%; the estimated mass was used to calculate the physical parameters with the “Physics properties” tool from SolidWorks.

The joint-trajectory-controller of the ROS2 control package has been implemented to control the manipulator. In turn, a PID controller has been implemented to control the drone, manually adjusting the gains online using a graphical user interface (GUI) developed in this work. In the experimental tests, the ability of SAMBot to remain hovering while extending and retracting the manipulator was analyzed, and basic movements in x, y, z, and yaw were performed. The results are shown in the following section.

3 RESULTS AND DISCUSSIONS.

The design of SAMBot is shown in Figures 3 and 4. Its design is symmetrical and takes advantage of the spherical structure so that the manipulator is part of it.

The previous section mentioned the sensors and actuators that will be used when applied in a real environment. The dimensions were checked carefully by using precision instruments, and the most relevant parts were printed for assembly tests. These elements are shown in Figure 5.

Our design was coupled with the Parrot AR Drone 2.0 in Gazebo to perform the simulations, as shown in Figure 6.

The GUIs were used to send control commands to the Drone and manipulator. The most relevant part is highlighted in green in Figure 7; from there, the PID gains were adjusted online to stabilize the Drone.

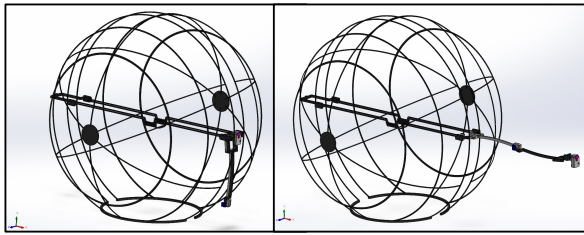


Figure 3: SAMBot design. Manipulator folded (left) and deployed (right).

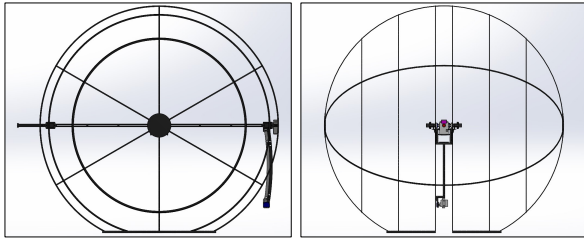


Figure 4: Side (left) and front (right) view of SAMBot with folded manipulator.

Figure 8 shows the error signals for x, y, z, and yaw when sending a command sequence to the Drone. The blue line is the current error, and the dashed red line indicates the zero error reference for an ideal case. The sequence is described below following the numbering marked in Figure 8:

1. A take-off signal was sent to the Drone to reach a reference of 2 m along the z-axis while the manipulator was retracted to its initial position (as seen in Figure 6). This action affected the x and z axes. In both cases (mainly for x), it was more difficult to reach the reference; however, the system did not present oscillations that affected its stability.
2. The manipulator was ordered to be fully deployed while the Drone remained hovering. Since the PID parameters were primarily tuned for this case, the error is nearly zero in all plots.
3. When the manipulator was folded back home, a behavior similar to that of point (1) was observed.

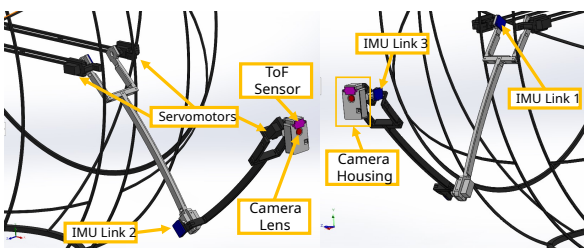


Figure 5: Assembly of sensors and actuators..

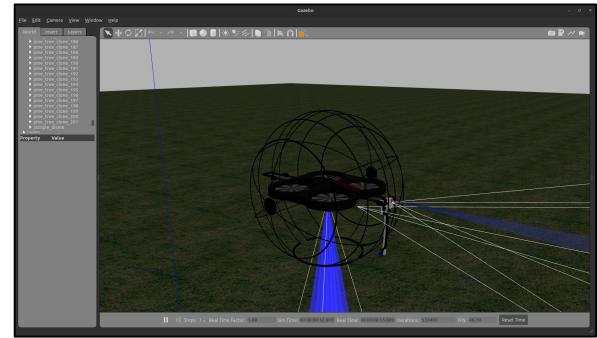


Figure 6: SAMBot simulation environment in Gazebo.

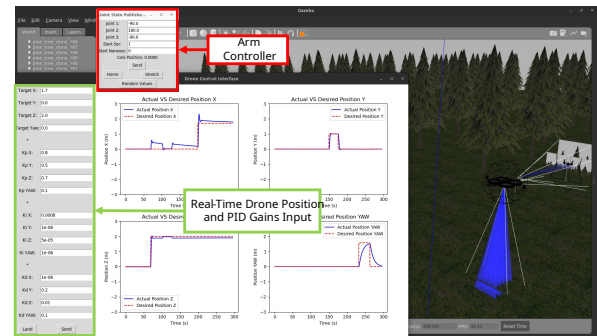


Figure 7: SAMBot simulation environment in Gazebo with GUI's for tuning and control.

4. It moved one meter in the positive direction of the y-axis. The error graph shows that the error decreases rapidly without considerable oscillations.
5. The same movement as the previous point, but this time in a negative sense.
6. Positive motion in yaw of 1.57 rad.
7. Negative movement in yaw of -1.57 rad relative to its current position. The graph shows that the yaw error tends practically to zero in stationary state.
8. Finally, the Drone is moved 1.3 meters towards the front (on the x-axis), and it was observed to have small oscillations until reaching a stationary error.

A similar sequence is illustrated in Figure 9, this time comparing the system's desired position with its actual position. The graphs show that the signals on the x and z axes are similar when the manipulator is fully folded, as shown in (a), compared to when it is fully deployed, as shown in (b). Some screenshots of the system are shown in Figure 10 while the simulation was running. A video of the simulation described above can be found at <https://www.youtube.com/watch?v=LFM5YPpHYyM>.

http://www.imavs.org/

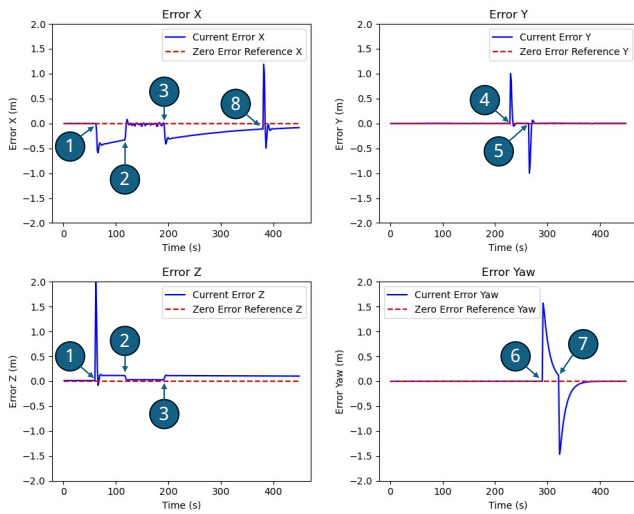


Figure 8: Error signals of x, y, z, yaw during a sequence of commands sent to the Drone.

4 CONCLUSION

The design of “SAMBot: Spherical Aerial Manipulator Robot” has been presented, a novel system consisting of a mini-drone protected by a spherical structure and equipped with a manipulator. The protection provided by the sphere and the ability of the manipulator to access confined spaces allows our robot to expand to various applications, such as accessing complex forest environments to obtain information on crops, search and rescue in mines or collapsed buildings, infrastructure inspection, autonomous underground navigation, among others. In our extensive research, we found a surprising gap in the literature—no studies on similar robots. This stark absence underlines the pressing need for research on applications of spherical drones with manipulation capabilities. As a contribution to this field, we have incorporated our design into Gazebo in ROS2 Humble, and it will be freely available to researchers who wish to delve into this unexplored area of research. A PID controller has been implemented to stabilize the Drone. We have developed a graphical user interface (GUI) that allows users to manually adjust the gains online. In future work, we will implement more complex control strategies, such as Robust or Adaptive Control combined with Artificial Intelligence strategies, to compensate for the manipulator’s dynamic movement and the moment of inertia generated by our complete system.

REFERENCES

[1] Mostafa Hassanalain and Abdessattar Abdelkefi. Classifications, applications, and design challenges of drones: A review. *Progress in Aerospace sciences*, 91:99–131, 2017.

[2] J Daniel Olivares-Figueroa, Israel Cruz-Vega, JM Ramírez-Cortés, P Gómez-Gil, and J Martínez-

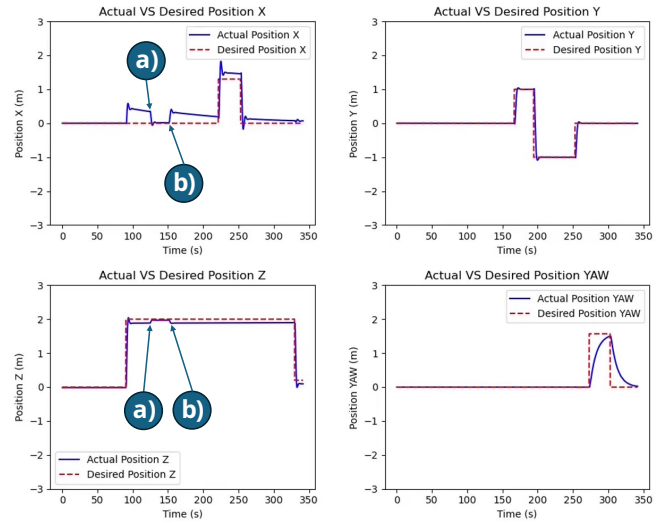


Figure 9: Desired position vs actual position signals.

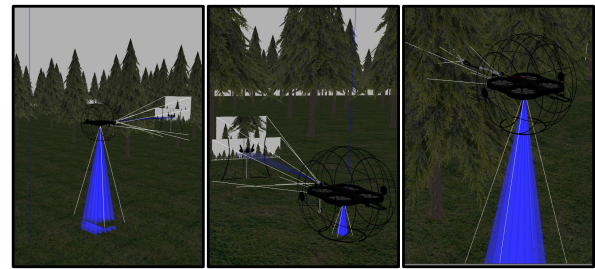


Figure 10: SAMBot simulation images.

Carranza. A compact approach for emotional assessment of drone pilots using bci. In *12th international micro air vehicle conference, Puebla, México*, pages 57–62, 2021.

[3] S Ahirwar, R Swarnkar, S Bhukya, and G Namwade. Application of drone in agriculture. *International Journal of Current Microbiology and Applied Sciences*, 8(01):2500–2505, 2019.

[4] Gopal Dutta and Purba Goswami. Application of drone in agriculture: A review. *International Journal of Chemical Studies*, 8(5):181–187, 2020.

[5] Mohammad Fatim Fatihur Rahman, Shurui Fan, Yan Zhang, and Lei Chen. A comparative study on application of unmanned aerial vehicle systems in agriculture. *Agriculture*, 11(22), 2021.

[6] João Valente, Rodrigo Almeida, and Lammert Kooistra. A comprehensive study of the potential application of flying ethylene-sensitive sensors for ripeness detection in apple orchards. *Sensors*, 19(2):372, 2019.

http://www.imavs.org/

- [7] Salua Hamaza, Ioannis Georgilas, Manuel Fernandez, Pedro Sanchez, Thomas Richardson, Guillermo Heredia, and Anibal Ollero. Sensor installation and retrieval operations using an unmanned aerial manipulator. *IEEE Robotics and Automation Letters*, 4(3):2793–2800, 2019.
- [8] André Farinha, Raphael Zufferey, Peter Zheng, Sophie F. Armanini, and Mirko Kovac. Unmanned aerial sensor placement for cluttered environments. *IEEE Robotics and Automation Letters*, 5(4):6623–6630, 2020.
- [9] Kenjiro Tadakuma, Carl John Salaan, Eri Takane, Yoshito Okada, Kazunori Ohno, and Satoshi Tadokoro. Design of aerial manipulator suitable for a uav with two passive rotating hemispherical shells. In *2018 IEEE International Symposium on Safety, Security, and Rescue Robotics (SSRR)*, pages 1–6, 2018.
- [10] Adrien Briod, Przemyslaw Kornatowski, Jean-Christophe Zufferey, and Dario Floreano. A collision-resilient flying robot. *Journal of Field Robotics*, 31(4):496–509, 2014.
- [11] Javad Shahmoradi, Amir Mirzaeinia, Pedram Roghanchi, and Mostafa Hassanalian. Monitoring of inaccessible areas in gps-denied underground mines using a fully autonomous encased safety inspection drone. In *AIAA Scitech 2020 Forum*, page 1961, 2020.
- [12] Paolo De Petris, Huan Nguyen, Mihir Dharmadhikari, Mihir Kulkarni, Nikhil Khedekar, Frank Mascari, and Kostas Alexis. Rmf-owl: A collision-tolerant flying robot for autonomous subterranean exploration. In *2022 International Conference on Unmanned Aircraft Systems (ICUAS)*, pages 536–543. IEEE, 2022.
- [13] Shoma Mizutani, Yoshito Okada, Carl John Salaan, Takuma Ishii, Kazunori Ohno, and Satoshi Tadokoro. Proposal and experimental validation of a design strategy for a uav with a passive rotating spherical shell. In *2015 IEEE/RSJ International Conference on Intelligent Robots and Systems (IROS)*, pages 1271–1278, 2015.
- [14] Aldo Sollazzo, Armando Trento, and Efilena Baseta. Machinic agency - implementing aerial robotics and machine learning to map public space. *35th eCAADe Conference - Sharing Computational Knowledge*, 2:611–618, 2017.
- [15] P.M. Kornatowski, S. Mintchev, and D. Floreano. An origami-inspired cargo drone. In *2017 IEEE/RSJ International Conference on Intelligent Robots and Systems (IROS)*, pages 6855–6862, 2017.
- [16] Wataru Yamada, Kazuhiro Yamada, Hiroyuki Manabe, and Daizo Ikeda. isphere: self-luminous spherical drone display. In *Proceedings of the 30th annual ACM symposium on user interface software and technology*, pages 635–643, 2017.
- [17] Xu Wei-hong, Cao Li-jia, and Zhong Chun-lai. Review of aerial manipulator and its control. *Int. J. Robot. Control Syst*, 1(3):308–325, 2021.
- [18] Xiangdong Meng, Yuqing He, Qi Li, Feng Gu, Liying Yang, Tengfei Yan, and Jianda Han. Contact force control of an aerial manipulator in pressing an emergency switch process. In *2018 IEEE/RSJ International Conference on Intelligent Robots and Systems (IROS)*, pages 2107–2113. IEEE, 2018.
- [19] Guangyu Zhang, Yuqing He, Bo Dai, Feng Gu, Jianda Han, and Guangjun Liu. Robust control of an aerial manipulator based on a variable inertia parameters model. *IEEE Transactions on Industrial Electronics*, 67(11):9515–9525, 2019.
- [20] Yen-Chen Liu and Chi-Yu Huang. Ddpq-based adaptive robust tracking control for aerial manipulators with decoupling approach. *IEEE Transactions on Cybernetics*, 52(8):8258–8271, 2021.
- [21] Weixuan Zhang, Maximilian Brunner, Lionel Ott, Mina Kamel, Roland Siegwart, and Juan Nieto. Learning dynamics for improving control of overactuated flying systems. *IEEE Robotics and Automation Letters*, 5(4):5283–5290, 2020.
- [22] Karen Bodie, Maximilian Brunner, Michael Pantic, Stefan Walser, Patrick Pfändler, Ueli Angst, Roland Siegwart, and Juan Nieto. Active interaction force control for contact-based inspection with a fully actuated aerial vehicle. *IEEE Transactions on Robotics*, 37(3):709–722, 2020.
- [23] Kyunam Kim, Patrick Spieler, Elena-Sorina Lupu, Alireza Ramezani, and Soon-Jo Chung. A bipedal walking robot that can fly, slackline, and skateboard. *Science Robotics*, 6(59):eabf8136, 2021.
- [24] Dimitris Chaikalis, Farshad Khorrami, and Anthony Tzes. Adaptive control approaches for an unmanned aerial manipulation system. In *2020 International Conference on Unmanned Aircraft Systems (ICUAS)*, pages 498–503. IEEE, 2020.
- [25] Yaqi Wu, Jin Song, Jiabi Sun, Fenfang Zhu, and Haoyao Chen. Aerial grasping based on vr perception and haptic control. In *2018 IEEE International Conference on Real-time Computing and Robotics (RCAR)*, pages 556–562. IEEE, 2018.

- [26] Yanjie Chen, Weiwei Zhan, Bingwei He, Lixiong Lin, Zhiqiang Miao, Xiaofang Yuan, and Yaonan Wang. Robust control for unmanned aerial manipulator under disturbances. *Ieee Access*, 8:129869–129877, 2020.
- [27] Joshua Fishman, Samuel Ubellacker, Nathan Hughes, and Luca Carlone. Dynamic grasping with a” soft” drone: From theory to practice. In *2021 IEEE/RSJ International Conference on Intelligent Robots and Systems (IROS)*, pages 4214–4221. IEEE, 2021.
- [28] Dimos Tzoumanikas, Felix Graule, Qingyue Yan, Dhruv Shah, Marija Popovic, and Stefan Leutenegger. Aerial manipulation using hybrid force and position nmpc applied to aerial writing. *arXiv preprint arXiv:2006.02116*, 2020.
- [29] Z Samadikhoshkho, S Ghorbani, F Janabi-Sharifi, and K Zareinia. Nonlinear control of aerial manipulation systems. *Aerospace Science and Technology*, 104:105945, 2020.
- [30] Karen Bodie, Maximilian Brunner, Michael Pantic, Stefan Walser, Patrick Pfändler, Ueli Angst, Roland Siegwart, and Juan Nieto. An omnidirectional aerial manipulation platform for contact-based inspection. *arXiv preprint arXiv:1905.03502*, 2019.
- [31] Emre Yilmaz, Hammad Zaki, and Mustafa Unel. Non-linear adaptive control of an aerial manipulation system. In *2019 18th European control conference (ECC)*, pages 3916–3921. IEEE, 2019.
- [32] Chioniso Kuchwa-Dube and Jimoh O Pedro. Quadrotor-based aerial manipulator altitude and attitude tracking using adaptive super-twisting sliding mode control. In *2019 International Conference on Unmanned Aircraft Systems (ICUAS)*, pages 144–151. IEEE, 2019.
- [33] James R Kutia, Karl A Stol, and Weiliang Xu. Aerial manipulator interactions with trees for canopy sampling. *IEEE/ASME transactions on mechatronics*, 23(4):1740–1749, 2018.
- [34] Vinh Nguyen, Anton Saveliev, and Andrey Ronzhin. Mathematical modelling of control and simultaneous stabilization of 3-dof aerial manipulation system. In *International Conference on Interactive Collaborative Robotics*, pages 253–264. Springer, 2020.
- [35] Chang Zhiyuan, Luo Yanyang, Shao Yanhua, Chu Hongyu, Wu Bin, Huang Mingqi, and Yunbo Rao. Fuzzy sliding mode control for rotorcraft aerial manipulator with extended state observer. In *2020 Chinese Automation Congress (CAC)*, pages 1710–1714. IEEE, 2020.
- [36] Dongjae Lee, Hoseong Seo, Inkyu Jang, Seung Jae Lee, and H Jin Kim. Aerial manipulator pushing a movable structure using a dob-based robust controller. *IEEE Robotics and Automation Letters*, 6(2):723–730, 2020.
- [37] Guangyu Zhang, Yuqing He, Bo Dai, Feng Gu, Liying Yang, Jianda Han, and Guangjun Liu. Aerial grasping of an object in the strong wind: Robust control of an aerial manipulator. *Applied Sciences*, 9(11):2230, 2019.
- [38] Xitong Guo, Pingjuan Niu, Di Zhao, Xia Li, Shan Wang, and An Chang. Model-free controls of manipulator quadrotor uav under grasping operation and environmental disturbance. *International Journal of Control, Automation, and Systems*, 20(11):3689–3705, 2022.